Computers and Geotechnics
Manuscript Draft

Manuscript Number: COGE-D-13-00021R1

Title: 3D Numerical Model for Dynamic Loading Induced Multiple Fracture Zones around Underground Cavity Faces

Article Type: Research Paper

Keywords: Deep underground; Initial stress; Stress gradient; Coupled static and dynamic; Zonal disintegration

Abstract: Three dimensional numerical modelling was used to examine the fracture responses around cavities in rock masses experiencing the stress of excavation. In addition to the primary fracture zone in the near field, numerical modelling generated a second fracture zone in the far field, and an elastic non-fracture zone between the two fields, i.e., fracture and non-fracture zones occur alternately around a deep cavity. Further research illustrated that the dynamic loading and static stress gradient are two necessary precursors for far field fracture in the excavation process. Neither quasi-static loading nor homogeneous stress conditions can induce a far field fracture. A simple theory is introduced suggesting that multiple fracture zones occur during excavation due to both the initial stress gradient and the dynamic loading. This finding indicates that it may be possible to induce continuous rock fracture in deep underground rock masses by employing optimal excavation methods to generate multiple contiguous fracture zones.

Answers to the reviewers' comments

Dear reviewers:
Our manuscript (ID: COGE-D-13-00021) was revised according to your comments. We hope that our responses have classified each of your comments and can be of help to the improvement of our manuscript. We apologize for the troubles brought by our carelessness. We appreciate your constructive criticisms. This answer sheet lists the major changes and our reply to the reviewers' comments and recommendations.

Answer to reviewer #1

1. *Page 5: 'a possible'*

   Response: Page 5 'a possible' was added.

2. *Page 8: "surely this is a function of the constitute model, is it brittle behaviour or ductile behaviour?"*

   Response: It is brittle behavior, the secondary fracture zone results from the combination of a dynamic loading acting over a cavity and an ascending static initial stress around it. When the peak stress which results from the ascending static stress gradient field in conjunction with the descending dynamic loading in a zone is more than the failure criterion of rock material, another fracture zone in far field will be induced.

3. *Page 9: "This is a massive deviatory stress field, are you sure?"*

   Response: Yes, this is a massive deviatory stress field. The aim of this manuscript is to illustrate that the unloading process can induce rock failure, thus the extreme massive deviatory stress field exists. In the practical engineering, the massive deviatory stress field results from three principal stresses, for example, the three principal stresses of "mine-by" tunnel in Canadian Underground Research Laboratory are σ_1 = 60 MPa, σ_2 = 11 MPa, σ_3 = 45 MPa (σ_2 is along tunnel axis) [1]

4. *Page 11: "What happens for a realistic excavation of say 5 m diameter?"*

   Response: A realistic excavation of 6 m diameter tunnel is added in section 6 in the revised manuscript.

Answer to reviewer #2

General comments:

1) *"The authors describe a numerical model in order to illustrate, rather than demonstrate, how a combination of a dynamic load acting over the face of a cavity and ascending stress gradient around it will induce another stress peak zone ahead of the loading face".*

   Response: This is a very good comment. Because both the theoretical methods and laboratory tests are not straightforward to demonstrate the mechanism of the multiple fracture zones phenomenon, the aim of our research is to illustrate that the excavation process can induce zonal disintegration. We presented one possible explanation for this phenomenon. The numerical results indicated that the multiple fracture phenomena occur in the high initial stress zone with the dynamic loading disturbing and we are planning to verify the mechanism mathematically and experimentally in the future.

2) *I say 'illustrate' and not 'demonstrate' because both the cavity dimension (diameter from 0.1 to 2 m) and the stress distribution around the cavity (up to 60 MPa in the axial direction of advancing) are different from those related to usual underground cavities such as tunnels. So, it is very difficult to extend the results from the actual model to tunnels.*

   Response: In order to make this study more understandable, a realistic excavation of 6 m diameter tunnel is added as an example in section 6 of the revised manuscript now

3) *In order to make the study more understandable, the authors should be more explicative about the cavity. This reviewer has the following doubts about the cavity described by the authors:*
   + A small diameter (0.20 m) and large and increasing axial stress could correspond to a borehole. Nevertheless, the initial stress magnitude (60 MPa) indicates that it should be a very deep bore hole, up to 2000 m in depth. In this case, what is the dynamic load in the axis direction? Is it an explosive charge?

   + If the cavity diameter is 1 m, could we assume that it is the cuthole of a tunnel face advanced by drilling and blasting? In this case the dynamic loading would be the action of the explosive. Nevertheless, how can the greater value of the stress in the axial direction be explained?

   + There is an excavation which the model could represent in a realistic way: a vertical shaft with a diameter of 1 to 2 m excavated by drilling and blasting between two levels of a deep mine. In this case, the dynamic loading would be the blasting action and the relationship of horizontal stress (σx or σz) to vertical stress (σy) could be less than 1.

Response: Yes, in our paper, the dynamic load is the equivalent blast load, i.e., explosive charge loading. Recently, many of the tunnel and mines are constructed at depth up to 2 000 m, such as the gold mines of the TauTona and East Rand in South Africa are about 3 900 m and 3 585, respectively, the mine of Agnico-Eagle's LaRonde is about 3000, and the Jinping‖Hydropower diversion tunnels are constructed at depth of 1500-2250 m.

With the increase of tunnel depth in the mining and civil engineering projects, the initial stress in such depth mines or tunnels should be very high. Ahead of the working face, moving away from the cavity boundary, the stress tensor eventually returns to its initial in-situ state. Generally in deep rock mass, the three principal stresses are not equal, the stress along tunnel axis in some case can be the maximum, the intermediate or the minimum principal stress, for example, the three stresses of "mine-by" tunnel in Canadian Underground Research Laboratory are σ_1 = 60 MPa, σ_2 = 11 MPa, σ_3 = 45 MPa (σ_2 is along tunnel axis) [1]. In fact, the zonal disintegration phenomena are not induced in any condition in the deep mines, and some occurs ahead of the working face [2] and others in the circuference of the tunnel [3]. Our conclusion is that there is higher possibility of zonal disintegration in the maximum principal stress direction.

In addition, the deep mines are normally hard rock mine, and the main excavation method is drill-blast. Just like the reviewer's comment that the ratio of horizontal stress (σx or σz) to vertical stress (σy) could be less than 1. However, blast loading is acting in three dimensional stress field; in fact, the conclusion of this paper is that the multiple zones (zonal disintegration) phenomena are induced in the maximum principal stress direction, not necessarily in vertical or horizontal direction.

4) *After the values recorded in Table 1, the study is carried out by analysing only a homogeneous very strong rock mass. Could this phenomenon be produced in weak rock mass?*

Response: Normally, the deep underground rock is hard or middle hardness rock, the previous monitoring about zonal disintegration only was conducted in hard rock mines. Therefore, the present study is only carried out by analyzing very strong rock. We also are interested to know whether this phenomenon could be produced in weak rock mass, but at present, we only focus on the hard rock mass.

5) *"Another weakness of the paper is that authors show the importance of dynamic load against a quasi-static one for the generation of far field*

fractures. Nevertheless, they do not mention anything about the frequency of the vibrations producing by this dynamic load, and this is quite important in all problems involving dynamic loading through rock materials."

Response: This is really a good comment. For a dynamic loading process, frequency is a dominant factor, the frequency, especially the main frequency of the vibration will affect the results. In general, for an explosive charge loading, the principal frequency is about from tens of Hz to several hundreds of Hz, thus, in this paper, the dynamic loading period varies from 2 ms to 20 ms associated with to get different frequency. But the main aim of this paper paid attention to verify whether zonal phenomenon will be produced in the underground or not, thus we did not pay much attention for frequency effect. Further research is needed to study the effect of the frequency of vibrations on fracture zone.

6) *The Authors also establish some conclusions which are merely hypotheses that cannot be confirmed from the actual numerical model. For example, it is difficult to deduce what they claim about the excavation with roadheaders in strong rock from the model. As stated above, the initial stress state around the cavity does not reproduce the normal stress state around a horizontal tunnel.*

Response: Firstly, in this paper, the dynamic loading is explosive charge loading, i.e., we assumed the excavation method is drill-blast method. Secondly, in the real excavation, in general, for drill-blast method, the cross-section of the tunnel is excavated by numbers of blasting hole; the loading conducted in the tunnel boundary is the superposition of every blast hole, which is a very complex process. However, based on the previous publications [4, 5], the explosive charge loading can be simplified as a loading curve, and the equivalent loading curve load can be applied in the tunnel boundary [6]. Therefore, in this paper, to simplify the problem, the blast load was simplified as a triangular load in the boundary of the tunnel to simulate the blast excavation process. Thirdly, in the underground, cavity or even blast hole, around or in front of the working face, there exist initial stress, and the stress distribution law (especial for circular cavity) approximately follows the Kirsch equation [7].

7) *Finally I have to say that the explanation of the mathematical formulae on which the model is based is rather scarce and difficult to understand if the reader is not an expert.*

Response: More detail was added to explain the mathematical formulae of the model.

Comments on concrete parts:

Title

8) *The title should point out that it is a theoretical analysis based on a numerical model, as for example 'development of 3D numerical model for...' or 'through a 3D numerical model...'*

Response: The title was replaced by "3D Numerical Model for Dynamic Loading Induced Multiple Fracture Zones around Underground Cavity Faces".

Abstract

9) *There are some statements in the abstract that cannot be directly deduced from the analysis. It would be better to remove them from the abstract. For example, the following sentence is not clearly demonstrated (there is not any energy balance in the analysis):*
'If an excavation process can induce multiple fracture zones ahead of the working face, subsequent working loads only need to stress and fracture the non-fracture zone, which would minimize the amount of energy required for excavation'

Response: The sentence "If an excavation process can induce multiple fracture zones ahead of the working face, subsequent working loads only need to stress and fracture the non-fracture zone, which would minimize the amount of energy required for excavation" in the abstract was removed in the revised manuscript.

10) *In the same way, the authors should be less categorical in the following sentence because this is only a hypothesis:*
In conjunction with other excavation methods, the continuous mining of hard rock deep underground becomes possible.
Are they proposing to use roadheaders and blasting alternatively?

Response: The sentence "in conjunction with other excavation methods, the continuous mining of hard rock deep underground becomes possible." was removed in the revised manuscript.

1. Introduction

11) *In the following sentence, has it been proved? Is there any reference about it?*
'Where it occurs around the circumference of a tunnel, it is closely associated with tunnel support and squeezing phenomena'

Response: Reference [6] in the revised manuscript was added.

2. Description of rock material model

12) *"What is the meaning of the acronym DIF?" Equation (1) and (2) (now, 3 and 4) should be explained in more detail.*

Response: DIF means dynamic increasing factor, and more detail was added in section 2.

13) *Equations (1) and (2) should be explained in more detail. It is difficult to understand a model based only on these equations.*

Response: More statements were added to describe the model in the section 2 of the revised manuscript.

14) *The definition of some variables, such as* $\dot{\varepsilon}_0$ *and* $\dot{\varepsilon}$*, is missing.*

Response: $\dot{\varepsilon}_0$ is initial effective strain rate, and $\dot{\varepsilon}$ is the effective strain rate. They were added in the revised manuscript.

3. Equivalent excavation loading

15) *Authors should define* ρ_0 *in equation (3) (now 5).*

Response: ρ_0 is explosive density and it was added in the revised manuscript.

4. Underground excavation modes and stress initialisation

16) *Why do the authors use as 'a cavity' a vertical hole with a diameter of 1 m?*

Response: Firstly, in our paper, we chose the loading direction along vertical (along tunnel axis) in order to better present the numerical results. In fact, if we change the tunnel axis along horizontal, the results is similar. Secondly, just like the reviewer said that most of the real tunnel could not be 1 m, the diameter of real drill-hole is less than 1 m and the real underground tunnel is larger than 1 m, therefore, we applied the temperate diameter for numerical testes and hoped to get general results, and if we adopt larger diameter tunnel for simulation, it will cost more computational time.

17) *The magnitude of the excavation diameter influences the initial stress state around the cavity. The Authors should point out here that the influence of the radius is studied later in the paper. It is also important to point out that the rock mass simulated is very strong (after the geotechnical parameters recorded in Table 1) and consequently the behavior of the rock mass will become elastic near the cavity walls.*

Response: We added a real excavation tunnel later in the paper, and we pointed out that the rock is very strong in revised manuscript. When the loading peak is not high, such as 100 MPa, the behavior of the rock mass near the cavity walls is elastic deformation. We pointed out the elastic and plastic deformation in the revised manuscript (Figures).

18) *The authors should not say that the model 'is able to simulate' if the results are not directly compared with real measures.*

Response: 'is able to simulate' was replaced by "could simulate".

19) *In order to better understand the study, it would be interesting for the author to describe a real excavation similar to theoretical 'cavity' described in the paper.*

Response: A real underground tunnel excavation project was added in section 6 to describe the multiple fracture zones around cavity in the revised manuscript.

5. Numerical modelling of excavation process

20) *Caption of Figure 4 is wrong. The 'initial circumferential stress' is 'pcs', no 'pas'.*

Response: 'pas' was replaced by 'pcs'.

5.1. Dynamic loading under different initial stress states

21) *The magnitude of the initial stress field 60 MPa is rather high. It is equivalent to a depth of about 2000 m for a rock with a density of 27 kg/m3. On the other hand, a cavity radius of 0.50 m is rather low. Are these values related to a real case?*

Response: Firstly, the multiple fracture zones phenomenon only monitored in deep mine, where high initial stress is observed. Secondly, many of mines are constructed at the depth about 2 000 m, and have high initial stresses, such as, the three principal stresses of 'mine-by' tunnel in Canadian Underground Research Laboratory are σ_1 = 60 MPa, σ_2 = 11 MPa, σ_3 = 45 MPa (σ_2 is along tunnel axis) [1], and in Jinping Ⅱ hydropower project: $\sigma_{maximum}$ = 69.5 MPa $\sigma_{minimum}$ = 23 MPa [8]. Thirdly, a cavity radius of 0.5 m is just used as an example, not a real case; a real case was added in section 6 of the revised manuscript.

22) *Some of the combinations of the stresses are rather rare (for example a stress in y-direction of 60 MPa and only 10 MPa in σx and σz directions). Only stresses around a vertical shaft between two levels of a deep mine could be similar. On the other hand, only combinations in which $\sigma x = \sigma z < \sigma y/2$ produce fragmentation in the far field. The Authors should be more explicative.*

Response: In this paper, the y-direction is along the tunnel axis, and it is not particularly for vertical direction. The initial stress in the *y*-direction of 60 MPa and only 10 MPa in σ_x and σ_z direction is a massive deviatory stress field example. The high initial stress level only exists in deep mining, and zonal disintegration phenomenon is also only monitored in deep mines. Based on Mohr-Coulomb criterion, the higher confining stress leads to higher axial strength, between the near field and far field, the near field rock mass has higher axial compression strength than that in the far field rock mass. If the circumferential stress is too high, for example $\sigma_x=\sigma_z>\sigma_y/2$, the axial strength is too high so that it cannot induce rock fracture in the far field. More detail was added in the revised manuscript.

23) *The variable and the units should appear in the legends of Figures 6 and 7.*

Response: Variable and units were added in Figures 6 and 7.

5.2 Different loading with constant initial stress state

24) Authors should explain at this point that the period of 200 ms is in order to simulate a quasi-static load because this time is clearly too big to simulate the peak load produced by an explosive charge.

Response: We totally agree with the reviewer's comment that the period of 200 ms is a quasi-static load, and our purpose is to compare the dynamic load with quasi-static load, thus, increased the period to 200 ms in order to get a quasi-static load and not an explosive charge.

25) *Has the frequency of the vibration produced through the rock mass no influence? The Authors should explain this.*

Response: For a dynamic loading process, frequency is one of dominant factors, the frequency, especially; the main frequency of the vibration will influence the results. In general, for an explosive charge loading, the principal frequency is about from tens of Hz to several hundreds of Hz, thus, in this paper, the dynamic loading period are 2 ms and 20 ms in order to get different frequency. But the main aim of this paper pays attention to verify whether zonal phenomenon will be produced in the underground or not, thus we did not pay much attention for the frequency effect.

5.3 Cavity size effect on fracture

26) The Authors use different cavity diameters. Nevertheless, none of them is similar to the dimensions of a conventional tunnel. For this reason, it is difficult to understand some of the statements made by the authors .

Response: We think it is better to use a real excavation project to replace this section. Thus, this section was replaced by ‘Verifying zonal disintegration in the practical project’, and a real underground tunnel was presented.

6 Dynamic and static stress state around an advancing cavity face

27) *Figs 7 and 8 have the same caption.*

Response: Fig 7 and Fig 8 were not having the same caption, and caption of Figures 17 were changed.

28) *What is the value of the initial static stresses for the result showed in Fig. 18?*

Response: The value of the initial static stresses for the result showed in Figure 18 was added.

29) *The following sentence in the last paragraph is true and easy to accept:*
'This finding is significant since a far field stress peak zone might offer advantages during excavation and disadvantages in terms of supporting the excavation cavity'
Nevertheless, the following sentence is less clear and even it seems to be incoherent with respect to the previous one:
'Thus the finding that a far field stress peak zone can be generated while excavating the near field, contributes an innovative method whereby a far field stress zone can be used to assist with rock excavation and reduce or eliminate the need for safety support'.

Response: ‘Thus the finding that a far field stress peak zone can be generated while excavating the near field, contributes an innovative method whereby a far field stress zone can be used to assist with rock excavation and reduce or eliminate the need for safety support’ was deleted in the revised manuscript.

Conclusions

30) *The following statements cannot be directly deduced from the present study and thus the authors should delete them from the conclusions:*
'The finding contributes to the design of an optimal excavation method based on the initial stress state and excavation size, which can induce follow-up fracture zones around the circumference of cavity, then reduce support intensity'.
'Furthermore, the study findings demonstrate that it is possible to develop an alternative excavation method that involves the generation of fracture zones ahead of the working face to minimize excavation energy. If every dynamic loading process can cause multiple fracture zones ahead of the working face, the subsequent excavation process only needs to excavate the non-fracture

zone. Thus a new practical excavation method is expected to achieve continuous mining in hard rock mines'.

Response: "The finding contributes to the design of an optimal excavation method based on the initial stress state and excavation size, which can induce follow-up fracture zones around the circumference of cavity, then reduce support intensity." and "Furthermore, the study findings demonstrate that it is possible to develop an alternative excavation method that involves the generation of fracture zones ahead of the working face to minimize excavation energy. If every dynamic loading process can cause multiple fracture zones ahead of the working face, the subsequent excavation process only needs to excavate the non-fracture zone. Thus a new practical excavation method is expected to achieve continuous mining in hard rock mines" were deleted in the revised manuscript.

References

[1] Read R. 20 years of excavation response studies at AECL's Underground Research Laboratory. International Journal of Rock Mechanics and Mining Sciences. 2004;41(8):1251-75.

[2] Adams G, Jager A. Petroscopic observations of rock fracturing ahead of stope faces in deep-level gold mines. Journal of the South African Institute of Mining and Metallurgy. 1980;80(6):204-9.

[3] Shemyakin E, Fisenko G, Kurlenya M, Oparin V, Reva V, Glushikhin F, et al. Zonal disintegration of rocks around underground workings, Part 1: Data of in situ observations. Journal of Mining Science. 1986;22(3):157-68.

[4] Torano J, Rodríguez R, Diego I, Rivas JM, Casal MD. FEM models including randomness and its application to the blasting vibrations prediction. Computers and Geotechnics. 2006;33(1):15-28.

[5] Gibson R, Toksöz M, Dong W. Seismic radiation from explosively loaded cavities in isotropic and transversely isotropic media. Bulletin of the Seismological Society of America. 1996;86(6):1910-24.

[6] Lu W, Yang J, Chen M, Zhou C. An equivalent method for blasting vibration simulation. Simulation Modelling Practice and Theory. 2011;19(9):2050-62.

[7] Brady BH, Brown ET. Rock mechanics: for underground mining: Springer, 2007.

[8] Qian Q, Zhou X, Yang H, Zhang Y, Li X. Zonal disintegration of surrounding rock mass around the diversion tunnels in Jinping II Hydropower Station, Southwestern China. Theoretical and Applied Fracture Mechanics. 2009;51(2):129-38.

3D Numerical Model for Dynamic Loading Induced Multiple Fracture Zones around Underground Cavity Faces

Ming Tao[a, b], Xibing Li[a *], Chengqing Wu[b]

[a]School of Resources and Safety Engineering, Central South University, Changsha, Hunan, PR, China

[b]School of Civil, Environmental and Mining Engineering, The University of Adelaide, SA, Australia

Ming Tao

E-mail: mtao211@gmail.com

[*]Corresponding author: Xibing Li

E-mail: xbli@mail.csu.edu.cn; Tel. /fax: +867318836450

Abstract: Three dimensional numerical modelling was used to examine the fracture responses around cavities in rock masses experiencing the stress of excavation. In addition to the primary fracture zone in the near field, numerical modelling generated a second fracture zone in the far field, and an elastic non-fracture zone between the two fields, i.e., fracture and non-fracture zones occur alternately around a deep cavity. Further research illustrated that the dynamic loading and static stress gradient are two necessary precursors for far field fracture in the excavation process. Neither quasi-static loading nor homogeneous stress conditions can induce a far field fracture. A simple theory is introduced suggesting that multiple fracture zones occur during excavation due to both the initial stress gradient and the dynamic loading. This finding indicates that it may be possible to induce continuous rock fracture in deep underground rock masses by employing optimal excavation methods to generate multiple contiguous fracture zones.

Keywords: Deep underground; Initial stress; Stress gradient; Coupled static and dynamic; Zonal disintegration

1 Introduction

Underground rock or ore are naturally stressed and deformed by their mass and volume. In a rock mass, therefore, when rock is excavated, stresses already existing in the rock mass are disturbed, leading to the redistribution of the primary in-situ stress field. The redistribution changes the magnitude of the stress-field tensor in the proximity of the excavation tunnel boundary, providing valuable information on the stability of the tunnel. Thus, the deformation ahead of and behind the advancing tunnel face is one of the most important topics in civil and mining engineering [1]. Research into both shallow and deep excavation engineering is therefore ongoing, and interesting and important differences have been observed in the behaviour of the rock mass at different levels of extraction.

In terms of deep underground excavation engineering, among other peculiar phenomena, zonal disintegration has emerged as an area of interest [2-4]. And since it was first recorded in the 1970s in the gold mines of the Witwatersrand in South Africa, experimental, theoretical and on site monitoring studies have been conducted to understand its full impact as a feature of deep underground rock mass behaviour. Zonal disintegration is characterized by its location around or in front of the working face [5], and has now been discovered in many locations, such as in deep underground mines in South Africa, Russia and China [3, 6]. When it occurs, fracture zones and non-fracture zones alternate around deep excavation cavities (Figure 1).

[Figure 1]

Conventional theoretical models related to deep cavities, however, indicate that the deformation and displacement are continuous; i.e., there are no alternating fracture zones. Therefore, zonal disintegration does not fit in the framework of the conventional theoretical models which assume that a mine shaft is surrounded by a zone of fractured or weakened rock in a state of critical equilibrium [7]. Thus, the reality of zonal disintegration offers a puzzle and a new way of understanding deep rock mechanisms and behaviours.

Verifying the mechanism of zonal disintegration and understanding of how it works and its implications in tunnelling has continued to challenge researchers in rock and mining engineering for the last 40 years. Zonal disintegration has become an important aspect of the development of discontinuous geomechanics. Where it occurs around the circumference of a tunnel, it is closely associated with tunnel support and squeezing phenomena [6]. On the other hand, where it occurs in front of the working face, especially for deep exploitation of hard rock metal mines, Li et al. [8, 9] suggest that the fractured zones ahead of the working face can be used to minimise excavation energy and enable continuous mining. However, there is still not a convincing explanation of zonal disintegration, and its mechanism continues to be debated [10].

Onsite monitoring has resulted in observations of zonal disintegration after excavation, which has resulted in the view that zonal disintegration is a static phenomenon [11]. However, this conclusion ignores the relationship of the high vertical and horizontal static stresses and the dynamic loading process initiated by different types of excavation, such as blasting and TBM. Deep underground excavation introduces forces that produce a complex, coupled static and dynamic situation, with conditions at the underground working face very different from the normal ground state, in terms of the mechanical behavior of the rock mass.

Based on the coupled static and dynamic Hopkinson bar, Li et al. [8] demonstrated that under coupled loads rock behaves differently compared to material subjected separately to either static or impact loading. However, on the working face (i.e., in the near-field), the stress tensor is very small. Ahead of the working face, moving away from the cavity boundary, the stress tensor eventually returns to its initial in-situ state (i.e, in the far-field) [12]. Therefore, the coupling of the initial static and dynamic loading cannot perfectly describe the nature of the loading around an underground working face, because the initial static stress exhibits gradient and stress fields that are highly inhomogeneous.

Given the complexity of the rock behaviour, initial stress distribution and dynamic loading have been two different research directions in the field of zonal disintegration. Guzev and Paroshin [13], for example, described the stress-field distribution around the underground

working face, and verified that disintegration zones can be identified using aspects of the rock parameters. Carter et al. [14, 15] analysed the size and stress gradient effects on rock fracture around cavities, and indicated that the initiation of stress for fracturing types depends on the cavity size and the associated stress gradient. Zhou et al. [16] got stress and displacement solutions for dynamic loading in plane strain conditions using the potential function.

These theoretical solutions, however, deal separately with either initial static stress fields or dynamic loading fields, and do not correspond sufficiently with underground excavation conditions, which involve simultaneous static and dynamic loading. In addition, there is no analytically solution available for stress and deformation redistribution problems in three dimensional (3D) states. The plane-strain elastic stress and displacement occurring around a circular tunnel located in a stress field are given by the Kirsch equation [17]. However, ahead of the working face, the radial stress and displacements around the circular opening were not obtained. Around the cavity's face, both stress fields and rock materials are highly inhomogeneous. Therefore, it is also not straightforward to get an analytically solution of a dynamic load equation around a deep underground tunnel, not to mention coupled static and dynamic loading.

Numerical analysis methods are popular and powerful tools for modelling brittle materials. Based on plane-strain analytical theory, many researchers have carried out large numbers of finite element and finite difference studies on the stresses and displacements occurring near the face of a tunnel opening [18-20]. For 3D numerical approaches, Basarir [1] analysed radial displacements occurring near the face of a circular opening in a weak rock mass using FLAC3D. However, most of the numerical modelling separately analyses static stress and dynamic loading, and does not to mention dynamic loading propagating in the void having a stress gradient.

In the current study, the commercial finite element program, LS-DYNA, was employed to simulate the excavation process of rock under 3D stress. This paper describes the investigation of a hard-rock dynamic excavation process using a numerical modelling method.

The stress initialization and distribution process around the tunnel were simulated using a dynamic relaxation method prior to dynamic loading. The dynamic loading was input using an equivalent load curve. After the initialization process, the dynamic loading was loaded onto the cavity face. The results indicated that, as well as the near field rock fracture zone, another stress peak zone or even rock fracture zone occurred in the far field, an unprecedented observation, not considered in conventional engineering practical and theoretical models.

In the stress gradient field, the present study indicates that the far field rock mass has a greater possibility of being fractured than the near field rock mass during a dynamic loading process (e.g.blasting). It should be noted that a quasi-static loading cannot induce a far field fracture zone. Without a stress gradient, there is no loading that can induce a far field fracture zone. This finding is important in any attempt to understand underground rock fracture as part of an excavation process. Based on the finding, it should be possible to induce far field fracture in new excavations, considerably improving excavation efficiency. Meanwhile, the finding offers a possible convincing explanation of zonal disintegration phenomena.

2 Description of rock material model

The continuous surface cap model (CSCM), which is widely used in LS-DYNA for brittle materials, has been employed to model the rock in this study. The CSCM was proved suitable for use with rock in earlier studies by Tao et al. [21]. In this model, the shear failure and the compaction surfaces are “blended” together to form a “smooth” or “continuous” surface [22]. The material model includes an isotropic constitutive equation, yielding and hardening surfaces, a damage formulation to simulate the softening and the modulus reduction, and a rate effects formulation to express the increasing strength resulting from the strain rate [22]. The yield equation is expressed as

$$f\left(I_1, J_2, J_3, k\right) = J_2 - \Re^2 F_c F_f^2 \tag{1}$$

where I_1, J_2 and J_3 are the first, the second and the third invariant of the stress tensor, respectively, k is the cap hardening parameter, and $\Re$ is the Rubin three-invariant reduction

factor. F_c is the hardening cap; F_f is the shear failure surface, which is defined in terms of I_1 as

$$F_f(I_1) = \alpha - \lambda \exp^{-\beta I_1} + \theta I_1 \tag{2}$$

where the parameters of α, β, λ and θ are selected by fitting the model surface to strength measurements taken from tri-axial compression tests conducted on plain rock cylinders.

The cap moves to simulate the plastic volume change, expanding to simulate plastic volume compaction and contracting to simulate plastic volume expansion, referred to as dilation. In the context of dynamic loading, the plastic hardening and strain rate effect of the rock mass was considered in CSCM at each time step. The viscoplastic algorithm interpolates between the elastic trial stress σ_{ij}^{T} and the inviscid stress without rate effect. To set the viscoplastic stress with a rate effect, the following equation is used [23].

If pressure is tensile

$$DIF = \begin{cases} \left(\dfrac{\dot{\varepsilon}}{\dot{\varepsilon}_0}\right)^{1.016\delta_s} & for\ \dot{\varepsilon} \le 30 s^{-1} \\ \beta_s \left(\dfrac{\dot{\varepsilon}}{\dot{\varepsilon}_0}\right)^{1/3} & for\ \dot{\varepsilon} > 30 s^{-1}, \end{cases} \tag{3}$$

where, $\delta_s = 1/\left(10 + 6 f_t^{'} / f_t^{0}\right)$, $\log \beta_s = 7.112\delta_s - 2.33$, $f_t^0 = 10MPa$, ε is strain, $\dot{\varepsilon}_0 = 30 \times 10^{-6} s^{-1}$ is initial effective strain rate, $\dot{\varepsilon}$ is effective strain rate, $f_t^{'}$ is rock tensile strength, and DIF means dynamic increasing factor.

If the pressure is compressive

$$DIF = \begin{cases} \left(\dfrac{\dot{\varepsilon}}{\dot{\varepsilon}_0}\right)^{1.026\alpha_S} & for\ \dot{\varepsilon} \le 30 s^{-1} \\ \beta_s \left(\dfrac{\dot{\varepsilon}}{\dot{\varepsilon}_0}\right)^{1/3} & for\ \dot{\varepsilon} > 30 s^{-1}, \end{cases} \tag{4}$$

Where, $\alpha_S = 1/\left(5 + 9 f_c^{'} / f_c^0\right), \log \beta_s = 6.156\alpha_s - 2$, $f_c^0 = 10MPa$, $\dot{\varepsilon}_0 = 30 \times 10^{-6} s^{-1}$, $f_c^{'}$ is rock compressive strength.

The complete descriptions of the model can be found in the LS-DYNA keyword user's manual [23]. In addition, most deep mines are hard rock or medium-hard rock mine; therefore, in the present paper hard rock is applied to verify the dynamic response. The material properties of the rock mass are presented in table 1.

[Table 1]

3 Equivalent excavations loading

In underground excavation, drill-blast is still a common excavation technique for mining or civil engineering tunnelling. Currently, with the rapid development of explosion theory and computer technology, many numerical programs can simulate the explosive process. The commercial finite element program LS-DYNA has proved well-suited to the simulation of the dynamic processes of rock masses [24-26]. In addition, wanting a simple and practical equivalent to actual blast loading and real blasts, Toraño et al. [27], as well as other researchers [28], sought some simple and practical methods by which to simulate explosive detonation and the propagation of seismic waves. Based on the Chapman-Jouguet model, the parameters at the detonation front are guided by the widely known equation by [29]

$$p_D = \frac{\rho_0 D^2}{1+\gamma} \tag{5}$$

Where, p_D is the detonation pressure, D is detonation velocity, ρ_0 is explosive density, γ is the ratio of the specific heats for the detonation gases. The initial explosion pressure p_0 applied to the blast-hole wall is approximately half of the detonation pressure for couple charges [29].

$$p_o = \frac{\rho_0 D^2}{2(1+\gamma)} \tag{6}$$

In general for decoupled charges, the initial explosion pressure p_0 is approximately as [29]

$$p_o = \frac{\rho_0 D^2}{2(1+\gamma)}\left(\frac{a}{b}\right)^{2\gamma} \tag{7}$$

where a is the charge diameter, b is the blast-hole diameter, in general, the value of γ is 3.0.

In addition, the variation of pressure with time includes three processes: the rise of the load, the initial expansion of gases, and the outburst of gases. Based on the previous publications relating to blasting procedures [30, 31], the blast load can simplified as a triangular load, that is a load with only one peak. Therefore, the loading curve of peak pressure, together with variation time, is employed for dynamic loading in this study in the follow sections.

4 Underground excavation modes and stress initialisation

Underground rock excavation first encounters initial static stress followed by excavation disturbed stress. Therefore, excavation is carried out in a situation of stress redistribution, and stress initialization is a necessary precursor to further underground excavation. Thus, the numerical modelling processes suggested by the current study involve two parts: one is static stress initialization; the other is excavation loading.

Due to the symmetry of the excavation tunnel geometry and the initial stress, the infinite space equivalent by one eighth of 3 D finite element models was constructed and solved by using the LS-DYNA program. The cavity face advancement was assigned to the y axis. The model geometry and boundary conditions are shown in Figure 2. The symmetric outer boundaries of the model were constrained to prevent lateral deformations. The initial stresses

were applied to the outer horizontal and vertical boundaries by three orthogonal compressions σ_x, σ_y, σ_z, where different σ_x, σ_y, and σ_z represent different initial stresses.

To obtain the steady state initial stress required to solve this quasi-static problem, *dynamic relaxation*, a method of applying a preload provided by LS-DYNA, was used to perform the static stress initialization. After initialization, a database that updates the geometry and the stress history of the rock allows the values of the deformed shape, the pre-stress and strain in the rock to be reformulated.

[Figure 2]

The grid is increasing size away from the cavity working face; and at the vicinity of the face, a fine grid of elements, to increase the accuracy of the results in the most important area [Figure 2 (c)]. Convergence tests were then conducted to determine how many elements would be needed to achieve a reliable estimation by decreasing the size of the elements until the difference of the results between two consecutive element sizes is less than 5%. The convergence tests resulted in the section of the element number that was employed in the simulation.

Using the rock model illustrated in Figure 2, the diameter of real excavation bore hole and tunnel are decimeter level and meter level, respectively. Therefore, taking the radius of the cavity as R = 0.5 m to represent a moderate size firstly. For example, when the initial stresses in the x, y, and z directions are σ_x = 60 MPa, σ_y = 60 MPa, and σ_z = 60 MPa, respectively, the results of the initial stress state can be shown in Figure 3.

[Figure 3]

Herein, within about 1 diameter of the cavity distance is called near-field and beyond 1 diameter distance is called the far-field. Figure 3 illustrates the fact that the near-field stress in each direction around the cavity is small. Moving away from the cavity boundary, the stress eventually equals the initial stress of 60 MPa (i.e. far-field stress), which is approximately with the reality stress state around of the underground cavity. The results prove that the

model could simulate the initial stress state of the cavity underground, and include the stress gradient around the cavity boundary.

5 Numerical modelling of excavation processes

After the static stress initialization, the explicit code was written for dynamic loading processes. An equivalent blast loading curve and a command for calling the results of the initialization were added, while the node and element components were deleted because they are not required during the loading stage. Additional loading curves represent different excavation processes. Hence, the stress state of rock excavation process is coupled initial static stress and dynamic loading, sketched as follows in Figure 4.

[Figure 4]

5.1 Dynamic loading under different initial stress states

To simplify the problem, it is assumed that the excavation is only conducted in *y* axis direction along the advancing face of the cavity. The equivalent blast loading, represented by a pressure-time triangular curve with a loading peak of 2000 MPa, rising time of 1.0E-03 ms, and period of 2 ms was tested first, as shown in Figure 5.

[Figure 5]

Additionally, taking the radius of the cavity as R = 0.5 m again, the vertical stress in the *y* direction was set as σ_y = 60 MPa in conjunction with different circumferential stresses in the *x* and *z* directions, set as $\sigma_x = \sigma_z$ = 10 MPa, $\sigma_x = \sigma_z$ = 20 MPa, $\sigma_x = \sigma_z$ = 40 MPa and $\sigma_x = \sigma_z$ = 60 MPa to characterize the rock behaviors. The results of the dynamic loading tests are presented as follows

[Figure 6]

The results illustrated that dynamic loading caused rock fracture at the loading face (i.e., near field fracture) at the beginning of the excavation. The area was therefore designated the *primary fracture zone*. Significantly, once this initial fracture had occurred, the initial stress states induced further fracturing (i.e., far field fracture) over time, or influenced the

development of a plastic zone on the periphery of the loading face [Figure 6 (a) and (b)]. Coming sometime after the initial fracture, these areas of failure were termed *secondary fracture zones.* The blast loading, therefore, induced failure in multiple locations over time.

Significantly, an elastic zone was observed between the primary and secondary fracture zones, i.e., zonal disintegration. This phenomenon is a departure from the conventional practical or conventional theoretical engineering models, and indicates that the dynamic loading process induced multiple discontinuous rock fracture zones rather than single fracture zone. In addition, the secondary fracture zone gradually disappeared as the circumferential stress increased [Figure 6 (c) and (d)].

To verify the relationship between zonal disintegration and the initial static stress state, a test using a $\sigma_x = \sigma_z = 30$ MPa constant circumferential stress with a different axial stress and the same dynamic loading curve as in Figure 5 was conducted to test the rock fracture response, the results are presented as follows

[Figure 7]

The results indicated that the secondary fracture zone (i.e., far field fracture zones) occurred during some of the loading process, such as in Figure 7 (b), (c), and (d). As axial stresses increased, the secondary fracture zone became more serious. Based on the numerical test results analysis, two conclusions can be demonstrated. Firstly, the dynamic loading process can induce multiple fracture zones. Secondly, the secondary fracture zone only happens when there is a high ratio of axial stress to circumferential stress, and higher stress ratios lead to a greater possibility of the secondary fracture zone. Thus, the static stress state is a dominant factor of zonal disintegration phenomenon.

5.2 Different loadings with constant initial stress state

Dynamic loading induces rock fracture and contributes significantly to zonal disintegration. Therefore, to characterize the effect of the loading, a constant initial stress state was paired with different loading curves for a series of numerical modelling tests. The above tests indicated that axial stresses at $\sigma_y = 60$ MPa and circumferential stress states of $\sigma_x = \sigma_z = 10$

MPa can induce zonal disintegration under dynamic loading. However, it is unclear whether a static or quasi-static loading process can also induce zonal disintegration. Thus, increase the loading period to 20 ms and 200 ms, respectively, and the loading peak still as 2 000 MPa (the same as Figure 5). The tests were conducted on the rock model with σ_y = 60 MPa of axial stress and σ_x = σ_z = 10 MPa of circumferential stress. The results are illustrated in Figure 8:

[Figure 8]

Figure 8 shows that the same initial state and the same loading peak nevertheless induce different rock fracture responses. When the loading period is 20 ms, two rock fracture zones are generated with a less serious secondary fracture zone than when the loading period is 2ms in above tests. However, when the loading period is 200 ms, only one fracture zone induced.

When the loading period is 200 ms, the loading process is approximated as a quasi-static loading process. Comparing dynamic loading to quasi-static loading, the dynamic loading process produces a dynamic wave, while a quasi-static loading does not. As the loading period increases, dynamic loading gradually moves to a quasi-static state, i.e., when the period is 200 ms, the loading process is a quasi-static process. Therefore no dynamic wave is produced and so the loading energy does not propagate to the far field. The far field therefore has no coupling of dynamic loading and initial static stress. The results of the test indicate that dynamic loading is another dominant factor in zonal disintegration, i.e., only a dynamic excavation method can induce the second fracture zone in the far field during the excavation process. The loading, however, must not be over an extended period.

This can be tested by adjusting the peak magnitude to verify the rock response, increase the loading peak from 2 000 MPa to 4 000 MPa, and decrease from 2 000 MPa to 1 000 MPa, respectively. The test results are presented in Figures 9 and 10.

[Figure 9]

[Figure 10]

When σ_y=60 MPa and σ_x=σ_z=20 MPa, the higher peak value (4 000 MPa) loading process induces a more serious rock fracture than the above sections loading process (peak of 2 000 MPa). The higher peak value even induced a second fracture zone in the far field, which was not induced by the lower peak (2 000 MPa) loading process of the stress state is σ_y=60 MPa and σ_x=σ_z=60 MPa. A lower peak value (1 000 MPa) induced less rock fracture and did not induce far field fracture when σ_y = 60 MPa and σ_x = σ_z = 60 MPa. These results indicate that the higher the dynamic loading, the higher possibility of rock fractures in the far field.

6 Numerical simulation of zonal disintegration in a practical project

In the practical engineering, the principal stresses of deep rock mass are not equal and could have massive deviatory stress field. For example, Jinping II hydropower project at the upriver of the Yalong River is located in Sichun Province, Southwest of China [5]. There are four main diversion tunnels with diameter of 12-13 m that are constructed at depth of 1500-2300 m. The length of each tunnel is about 16.67 km. The rock material parameters around the tunnels are as follows: Young's modulus 3.0×10^4 MPa, Poisson's ratio 0.2, uni-axial compression strength 150 MPa, rock density 2.75×10^4 kg/m3 [32]. The maximum principal stress σ_y = 69.5 MPa (vertical direction), the intermediate principal stress σ_z = 42 MPa (horizontal direction, along tunnel axis), and the minimum principal stress σ_x = 23 MPa (horizontal direction). A series of engineering difficulties, such as high initial stress, rock burst, etc. was confronted and zonal disintegration phenomenon was also found around the tunnels [5]. Two of the tunnels were constructed by drill-blast method. The TBM excavation method was adopted for others. For the drill-blast method, the tunnels were divided by two steps, one was excavation of the upper half part, and the next step was to excavate the lower half part. Thus, to simplify the problem, a tunnel with diameter of 6 m is setup for tunnel excavation. The decoupled charge configuration was adopted, the charge diameter is 35 mm, the blast-hole diameter is 42 mm, the explosive density is 1000 kg/m^3, and detonation velocity is 3400 m/s. Thus, for the case of decoupled charge, based on the equation of (5) and (7), it was found that the parameter of the detonation front was p_D = 2890 MPa, and the explosion applied on the blast-hole was p_0 = 484 MPa, and the duration of the blasting

loading is from 0 to 2 ms. To compare the response in the *x*, *y*, *z* directions, the equivalent loading applied around and in front of the working face, respectively. A quasi-static loading process with the same loading peak was conducted to compare the dynamic loading results. The numerical results are presented in Figures 11 and 12.

[Figure 11]

[Figure 12]

The numerical results indicated that zonal disintegration was not induced in front face of the tunnel, but in the circumferential direction of the tunnel (see Figure 12), which agrees with the previous publication [5]. In addition, for the circumferential direction, the zonal disintegration is obviously in the *y*-axis direction but not in the *x*-axis direction. In the front face of the tunnel, the initial stress along the tunnel axis direction is σ_z = 42.11, and circumferential initial stresses are σ_y = 69.5 MPa and σ_x = 23 MPa, respectively, the maximum principal stress is not along the loading direction. But in the circumferential direction of the tunnel, the initial stress along the loading direction σ_y = 69.5 MPa corresponds with the circumferential initial stresses of σ_x = 23 MPa and σ_z = 42 MPa, and the maximum principal stress is along the loading direction. For σ_x = 23 MPa corresponding with the circumferential initial stresses of σ_y = 69.5 MPa and σ_z = 42 MPa, the maximum principal stress is also not along the loading direction. Thus, it can show that the maximum principal stress direction has higher possibility of zonal disintegration than others, which also agrees with the above numerical testes. Alternatively, the numerical results also indicated that zonal disintegration is induced in the dynamic process and not in the quasi-static process (see Figure 12). Thus, in such a high initial stress state, during the drill-blast excavation process there is the possibility of zonal disintegration,

7 Dynamic and static stress state around an advancing cavity face

The above numerical results indicate that the second fracture zone is between 1 and 4 diameters of the cavity in distance away from the cavity. In general, at a distance from the working face of about 2-4 times the excavation diameter, the stress and deformation are approximately ±5% of the final stress and strain value [17]. Thus, the second fracture zone occurred in the stress gradient zone.

The stress state of conventional theoretical models of 2D deformation of a circular cavity, usually provided in most experiments presented in Figure 13 [7, 17].

[Figure 13]

In Figure 13, p is the field stress; σ_{rr} is radial stress component; $\sigma_{\theta\theta}$ is the circumferential stress component; both σ_{rr} and $\sigma_{\theta\theta}$ are related to the generation of the opening [17]. Figure 13 illustrates the main features of the stresses distribution around the opening; that is, both the gradient of σ_{rr} and $\sigma_{\theta\theta}$ are ascending, and eventually reach the initial stress (far field stress).

The calculation of 3D stress or displacement components beyond the cavity boundary is a rather difficult problem mathematically. The present model of the 3D numerical modelling results indicated that along the cavity driving face, the axial stress gradually ascends and circumferential stress is approximately constant. Therefore, the initial 3D stress state around the cavity can be illustrated as in Figure 14.

[Figure 14]

The lateral coordinates represent the distance ahead of the advancing cavity face, and the longitudinal coordinates represent the magnitude of the initial stress. And, indeed, the axial stress exhibits a stress gradient.

Furthermore, because there is a stress gradient around the cavity, the dynamic loading wave that propagates in the rock composition is inhomogeneous. It is therefore not straightforward to get an analytically solution of the loading wave beyond the cavity boundary. However, it is obvious that the magnitude of the dynamic loading wave is gradually descending, and can be illustrated as in Figure 15.

[Figure 15]

Figure 16 reveals the coupled stress state ahead of the cavity working face.

[Figure 16]

Figure 16 shows that ahead of the working face, the ascending initial static stress and descending dynamic loading intersect at (*h*), forming two stress coupling zones, *A* and *B*. In zone *A*, the primary rock fracture zone will expend energy so that the magnitude of the loading gradually decreases. Meanwhile, as primary rock fracture progresses, the initial stress is redistributed again, ahead of the new cavity face caused by the behavior of the rock mass in the primary fracture zone, and a new stress gradient field is generated.

Activity in the primary rock fracture zone ceases when the magnitude of the dynamic loading, coupled with low initial static stress, becomes insufficient to induce rock fracture. However, a residual wave of dynamic loading continues to propagate along the *y* direction to the far field, gradually decreasing as the energy dissipates. Ahead of the primary fracture face, the stress state is coupled with the descending dynamic loading and ascending initial static stress. Thus, there must be another load peak after the intersection point, i.e., *B* zone will have another peak load value. Using a loading curve to describe the coupled stress state, the impact loading combined with initial stress can be demonstrated as in Figure 17.

[Figure 17]

Figure 17 illustrates the fact that coupling stresses have two high stress peak values. Assuming a certain stress level will cause rock fracture, and then the dotted line represents the rock fracture stress level, meaning that there are two zones where rock fracture could possibly be induced. The graph makes it clear why some of the numerical tests cause two rock fracture zones, while others do not. When the cavity size and axial stress are constant values, the higher circumferential stress means greater rock strength, which will cost more dynamic loading energy in the primary fracture zone. Therefore, when the dynamic load is a constant, the second coupling stress is not enough to induce rock fracture in high circumferential stress states. In addition, if the initial axial stress is low, and the stress gradient is lower, the coupling of the static and dynamic is also not enough to induce rock fracture. In these situations, neither lower axial stress nor higher circumferential stress can induce rock fracture.

On the other hand, if the loading is not dynamic, no wave propagates to the far field. There is, therefore, no dynamic loading coupling associated with static stress. In fact, the initial stress gradient and dynamic loading are necessary precursors of multiple rock fracture zones. Furthermore, if a new fracture zone occurs in the far field in association with new stress redistribution, it is possible to induce multiple peaks at the fracture zone. Therefore, the coupled stress state can be approximated as shown in Figure 18.

[Figure 18]

It is assumed that the strength of the rock mass is described by the Mohr-Coulomb criterion [17], i.e.

$$\sigma_1 = \sigma_3 \frac{1+\sin\phi}{1-\sin\phi} + \frac{2c\cos\phi}{1-\sin\phi} \tag{8}$$

where, σ_1 is the maximum principal stress and σ_3 is the minimum principal stress, c is cohesion, and ϕ is the angle of internal friction.

The main difference is that the far field rock mass exhibits higher initial axial stress than the near field rock mass. The circumferential stress component is approximately equal, however. Therefore, the near field rock mass needs more excavation energy (loading energy) than the far field rock mass, because the far field rock mass has higher initial static stress.

The evidence results in the hypothesis, therefore, that coupled dynamic loading and initial static stress induce far field fracture meaning that there should be a suitable dynamic loading magnitude that will induce rock fracture ahead of the working face but not in the working face. After many tests, the loading curve with 100 MPa loading peak verified the hypothesis. The results are graphically presented in Figure 19.

[Figure 19]

The results indicate that ahead of the working face have a rock fracture zone and rock fracture did almost not induce in the working face. Therefore, the inference of the coupled dynamic loading with static stress gradient is right.

The onsite monitor recorded several rock fracture zones, but the current study only generated a major fracture zone in far field. If fracture is induced in the second zone, the initial stresses will redistribute again and another stress gradient field zone is generated around the induced failure. When the resident dynamic loading is coupled with the new static stress, a new area of fracture is possible, but after many numerical tests, no other fracture zones were observed after the second one.

In practice, during engineering excavation, zonal disintegration or far field fracture zones cannot be observed directly unless a borehole camera or geophysical method is employed. Thus, it is not straightforward to determine whether the far field fracture zone is induced during the dynamic loading process or induced after a relatively long time of dynamic excavation. Furthermore, dynamic loading and initial static stress are necessary precursors to the development of the far field zone, thus, zonal disintegration or far field fracture is not a very common phenomenon underground. However, based on the findings of the current study, it can be concluded that an ascending stress gradient field in conjunction with a descending dynamic loading will induce another stress peak zone ahead of the loading face. This finding is significant since a far field stress peak zone might offer advantages during excavation and disadvantages in terms of supporting the excavation cavity.

Conclusions

The study reported here indicates that in the right conditions the dynamic loading process induces multiple fracture zones around underground cavities. Using a 3D finite element program, the study successfully simulated and proved that there is the possibility of fracture and non-fracture zones alternating around underground excavation working faces. In addition, the necessary precursors of alternating zones were also found in this study: high initial stress in the rock mass associated with a stress gradient and dynamic loading in the excavation process. The gradual attenuation of the dynamic loading couples with the initial static stress induced the far field stress peak zone and even fracture zone. Furthermore, the maximum principal stress direction has higher possibility of zonal disintegration than others. Previous studies have paid too much attention to the role of the primary rock fracture zone, and tended

to ignore the important role of far field stress peak zones in underground mining and civil engineering, thus, this finding presented a new way of understanding high initial stress rock mechanisms and behaviours.

Acknowledgments

The research presented in this paper was jointly supported by the 973 Program of China (grant No. 2010CB732004), the National Natural Science Foundation of China (grant No. 50934006, 10872218, and 11102239) The first author would like to thank the Chinese Scholarship Council for financial support to the joint PhD study at The University of Adelaide, Australia and express the acknowledgement to Mr. QianQian at The University of Adelaide and Mr. JiaLu Ma at Harbin Institute of Technology.

References

[1] Basarir H, Genis M, Ozarslan A. The analysis of radial displacements occurring near the face of a circular opening in weak rock mass. International Journal of Rock Mechanics and Mining Sciences 2010;47(5): 771-783.

[2] Adams GR, Jager AJ. Petroscopic observations of rock fracturing ahead of stope faces in deep-level gold mines. Journal of the South African institute of mining and metallurgy 1980. 80, 204-209.

[3] Shemyakin EI, Fisenko GL, Kurlenya MV, Oparin VN, Reva VN, Glushikhin FP, Rozenbaum MA, Tropp EA, Kuznetsov YD. Zonal disintegration of rocks around underground workings, Part 1: Data of in situ observations. Journal of Mining Science 1986; 22(3): 157-168.

[4] Zhou XP, Song HF, Qian QH. Zonal disintegration of deep crack-weakened rock masses: A non-Euclidean model. Theoretical and Applied Fracture Mechanics 2011;55(3): 227-236.

[5] Qian QH, Zhou XP, Yang HQ, Zhang YX, Li XH. Zonal disintegration of surrounding rock mass around the diversion tunnels in Jinping II Hydropower Station, Southwestern China. Theoretical and Applied Fracture Mechanics 2009;51(2): 129-138.

[6] Jia P, Yang TH, Yu QL. Mechanism of parallel fractures around deep underground excavations. Theoretical and Applied Fracture Mechanics 2012; 61: 57-65.

[7] Shemyakin EI, Fisenko GL, Kurlenya MV, Oparin VN, Reva VN, Glushikhin FP, Rozenbaum MA, Tropp EA, Kuznetsov YD. Zonal disintegration of rocks around underground mines, part III: theoretical concepts. Journal of Mining Science 1987; 23(1): 1-6.

[8] Li XB, Zhou ZL, Lok TS, Hong L, Yin TB. Innovative testing technique of rock subjected to coupled static and dynamic loads. International Journal of Rock Mechanics and Mining Sciences 2008;45(5): 739-748.

[9] Li XB, Yao JR, Gong FQ. Dynamic problems in deep exploitation of hard rock metal mines. The Chinese Journal of Nonferrous Metals 2011; 21(10): 2551-2563 [in Chinese].

[10] Tan YL, Ning JG, Li HT. In situ explorations on zonal disintegration of roof strata in deep coalmines. International Journal of Rock Mechanics and Mining Sciences 2012;49:113-124.

[11] Wu H, Fang Q, Zhang YD, Gong ZM. Zonal disintegration phenomenon in enclosing rock mass

surrounding deep tunnels—mechanism and discussion of characteristic parameters. Mining Science and Technology 2009;19(3): 306-311.
[12] Eberhardt E. Numerical modelling of three-dimension stress rotation ahead of an advancing tunnel face. International Journal of Rock Mechanics and Mining Sciences 2001;38(4): 499-518.
[13] Guzev MA, Paroshin AA. Non–euclidean model of the zonal disintegration of rocks around an underground working. Journal of Applied Mechanics and Technical Physics 2001;42(1): 131-139.
[14] Carter BJ, Lajtai EZ, Petukhov A. Primary and remote fracture around underground cavities. International Journal for Numerical and Analytical Methods in Geomechanics 1991;15(1): 21-40.
[15] Carter BJ. Size and stress gradient effects on fracture around cavities. Rock mechanics and rock engineering 1992;25(3): 167-186.
[16] Zhou XP, Wang FH, Qian QH, Zhang BH. Zonal fracturing mechanism in deep crack-weakened rock masses. Theoretical and Applied Fracture Mechanics 2008;50(1): 57-65.
[17] Brady BH, Brown ET. Rock mechanics: for underground mining: Springer, 2007.
[18] Abdel-Meguid M, Rowe RK, Lo KY. Three-dimensional analysis of unlined tunnels in rock subjected to high horizontal stress. Canadian geotechnical journal 2003;40(6): 1208-1224.
[19] Basarir H. Analysis of rock-support interaction using numerical and multiple regression modeling. Canadian geotechnical journal 2008;45(1): 1-13.
[20] Yavuz H. Support pressure estimation for circular and non-circular openings based on a parametric numerical modelling study. The Journal of The South African Institute of Mining and Metallurgy 2006;106(2): 129-138.
[21] Tao M, Li XB, Wu CQ. Characteristics of the unloading process of rocks under high initial stress. Computers and Geotechnics 2012;45, 83-92.
[22] Murray YD. Theory and Evaluation of Concrete Material Model 159. 8th International LS-DYNA Users Conference2004.
[23] LSTC. LS-DYNA keyword user's manual, version 971. Livermore softwave Technology Corporation2007;2206pp.
[24] Lu WB, Yang JH, Yan P, Chen M, Zhou CB, Luo Y, Jin L. Dynamic response of rock mass induced by the transient release of in-situ stress. International Journal of Rock Mechanics and Mining Sciences 2012;53: 129-141.
[25] Ma GW, An XM. Numerical simulation of blasting-induced rock fractures. International Journal of Rock Mechanics and Mining Sciences 2008;45(6): 966-975.
[26] Wei XY, Zhao ZY, Gu J. Numerical simulations of rock mass damage induced by underground explosion. International Journal of Rock Mechanics and Mining Sciences 2009;46(7): 1206-1213.
[27] Toraño J, Rodríguez R, Diego I, Rivas JM, Casal MD. FEM models including randomness and its application to the blasting vibrations prediction. Computers and Geotechnics 2006;33(1): 15-28.
[28] Gibson JrRL, Toksöz MN, Dong W. Seismic radiation from explosively loaded cavities in isotropic and transversely isotropic media. Bulletin of the Seismological Society of America 1996;86(6): 1910-1924.
[29] Lu WB, Yang JH, Chen M, Zhou CB. An equivalent method for blasting vibration simulation. Simulation Modelling Practice and Theory 2011;19(9): 2050-2062.
[30] Krauthammer T, Astarlioglu S, Blasko J, Soh TB, Ng PH. Pressure–impulse diagrams for the behavior assessment of structural components. International journal of impact engineering 2008;35(8): 771-783.
[31] Li QM, Meng H. Pressure-impulse diagram for blast loads based on dimensional analysis and single-degree-of-freedom model. Journal of engineering mechanics 2002;128(1): 87-92.
[32] Wu SY, Ren XH, Chen XR, Zhang JX. Stability analysis and supporting design of surrounding rocks of

diversion tunnel for Jinping hydropower station. The Chinese Journal of Nonferrous Metals. 2005;24(20):3777-3782 [in Chinese].

Figure titles

Figure

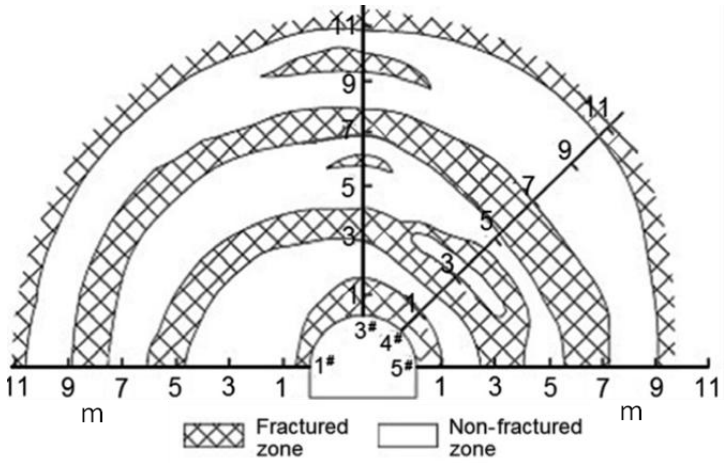

Figure 1 The zonal disintegration phenomenon of mine [3, 4]

Figure

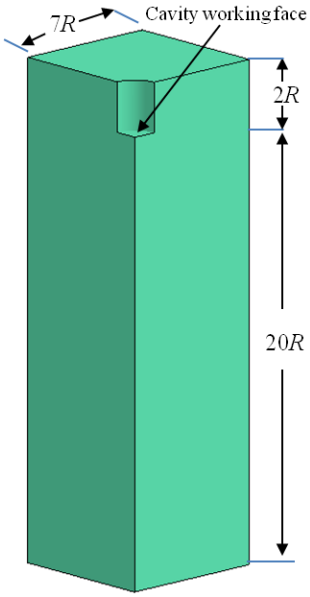

(*a*) oblique view

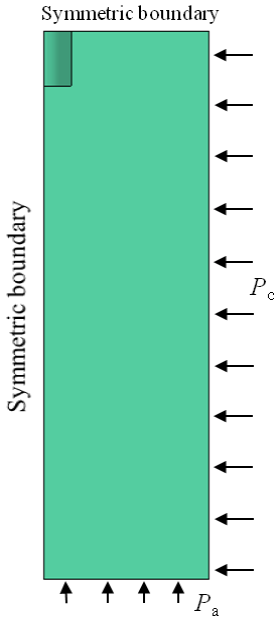

(*b*) fron view

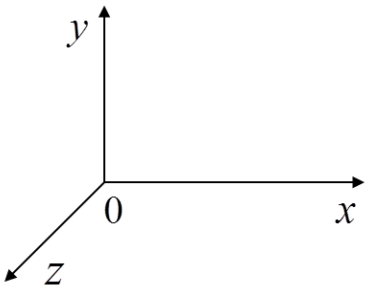

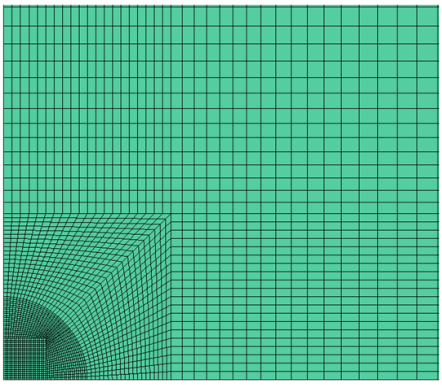

(*c*) top view and grid

Figure 2 Model geometry and boundary conditions

Figure

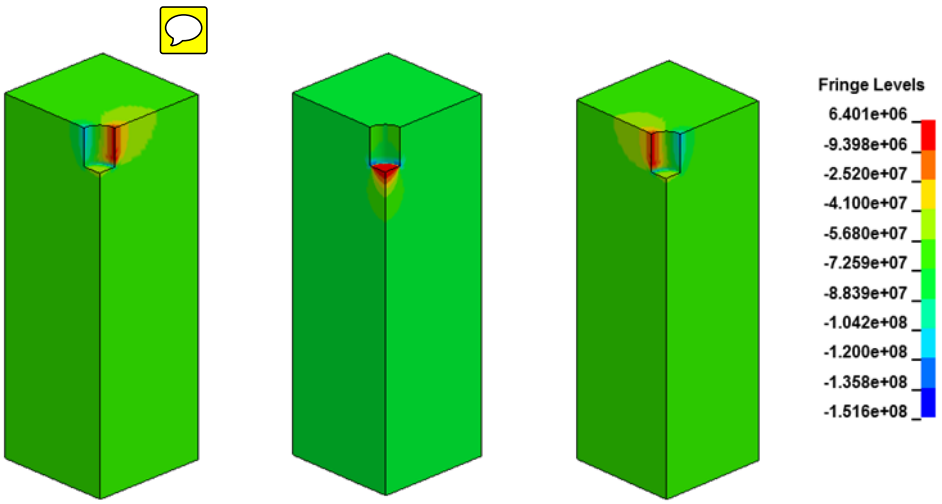

(*a*) *x* direction (*b*) *y* direction (*c*) z direction

Figure 3 Initial stress state in *x*, *y*, and *z* direction (Fringe levels are stress, pa)

Figure

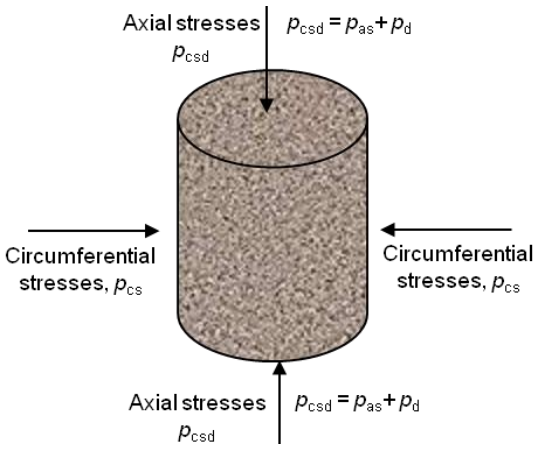

Figure 4 Schematic diagram of rock stress models at underground (p_{csd}: coupled static and dynamic loading; p_{as}: initial axial static stress; p_{cs}: initial circumferential stress; p_d: dynamic loading)

Figure

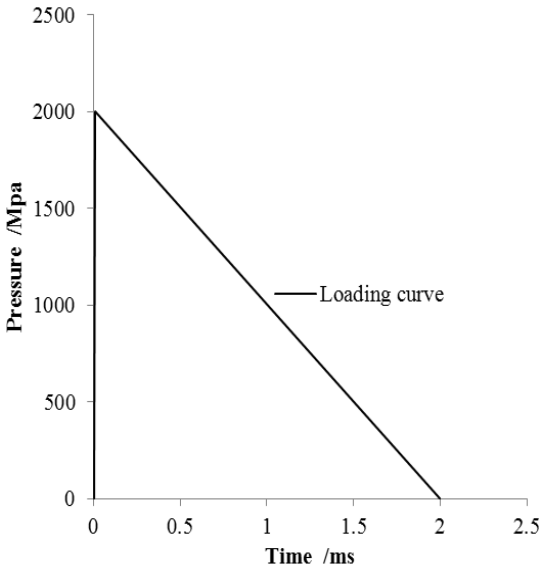

Figure 5 Dynamic loading curve

Figure

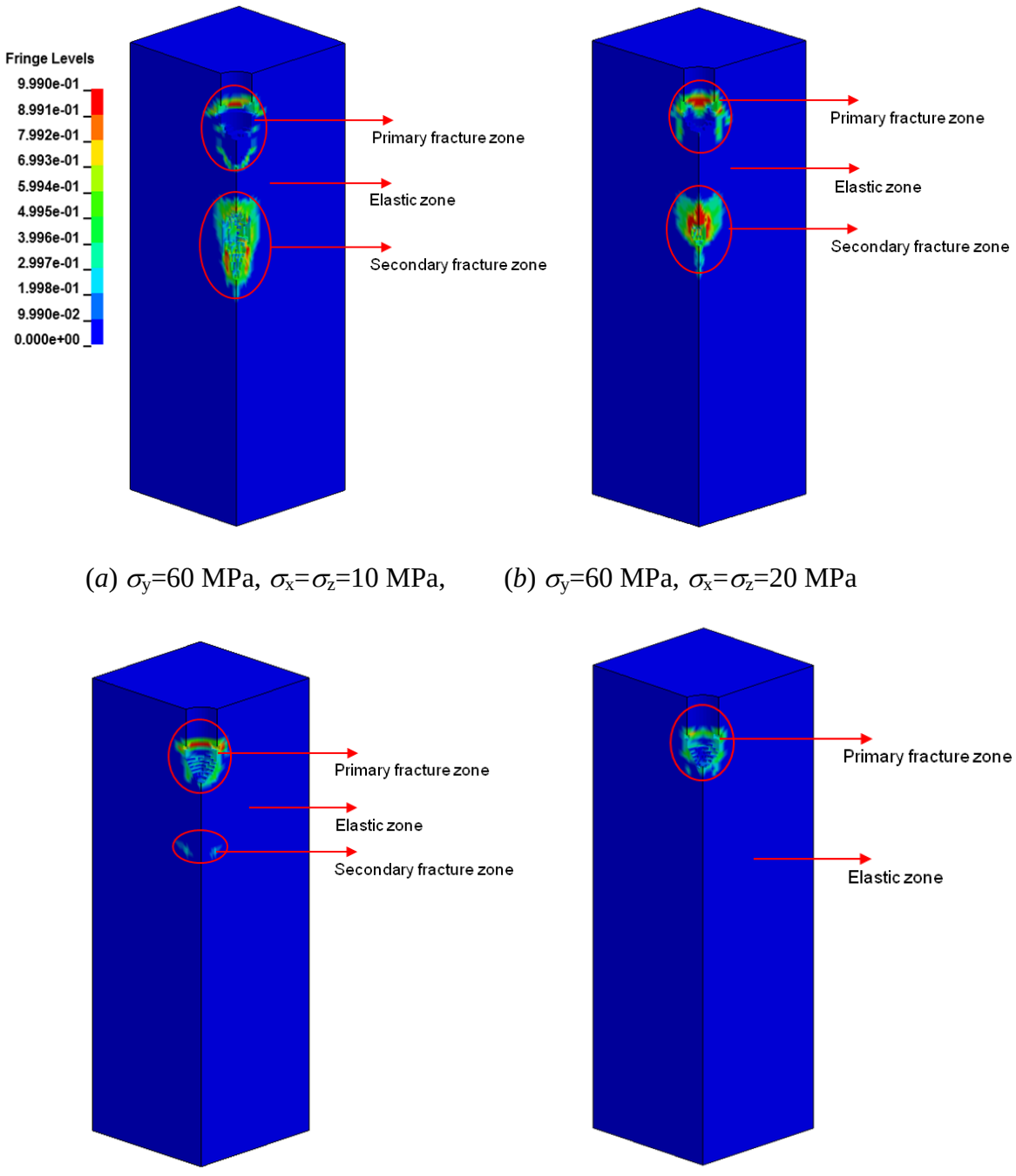

(*a*) σ_y=60 MPa, σ_x=σ_z=10 MPa, (*b*) σ_y=60 MPa, σ_x=σ_z=20 MPa

(*c*) σ_y=60 MPa, σ_x=σ_z=40 MPa, (*d*) σ_y=60 MPa, σ_x=σ_z=60 MPa

Figure 6 Blasting excavation process in different circumference initial stress states (Fringe levels are plastic strain)

Figure

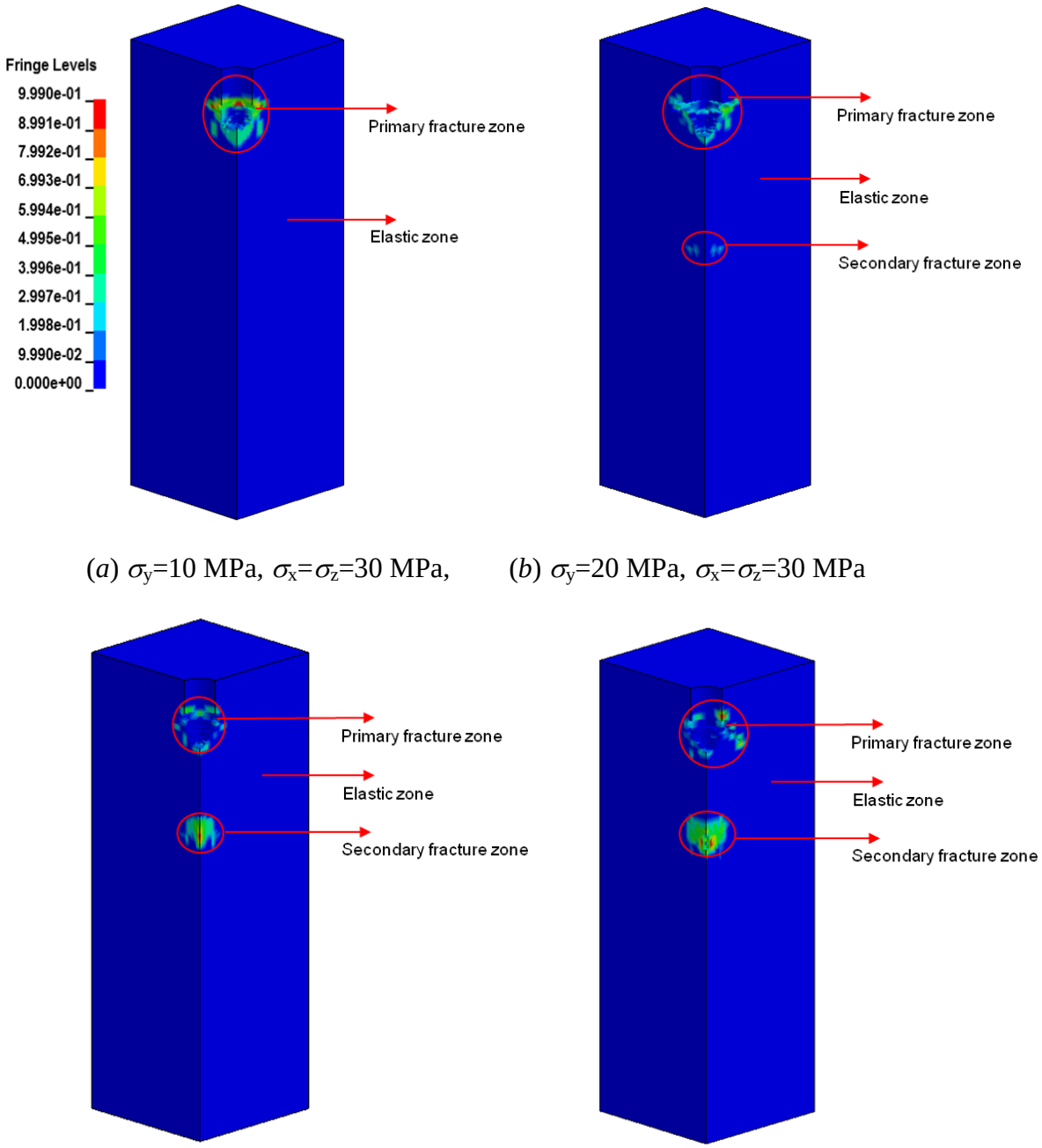

(*a*) σ_y=10 MPa, σ_x=σ_z=30 MPa, (*b*) σ_y=20 MPa, σ_x=σ_z=30 MPa

(*c*) σ_y=60 MPa, σ_x=σ_z=30 MPa, (*d*) σ_y=80 MPa, σ_x=σ_z=30 MPa

Figure 7 Dynamic loading processes in different axial initials stress states (Fringe levels are plastic strain)

Figure

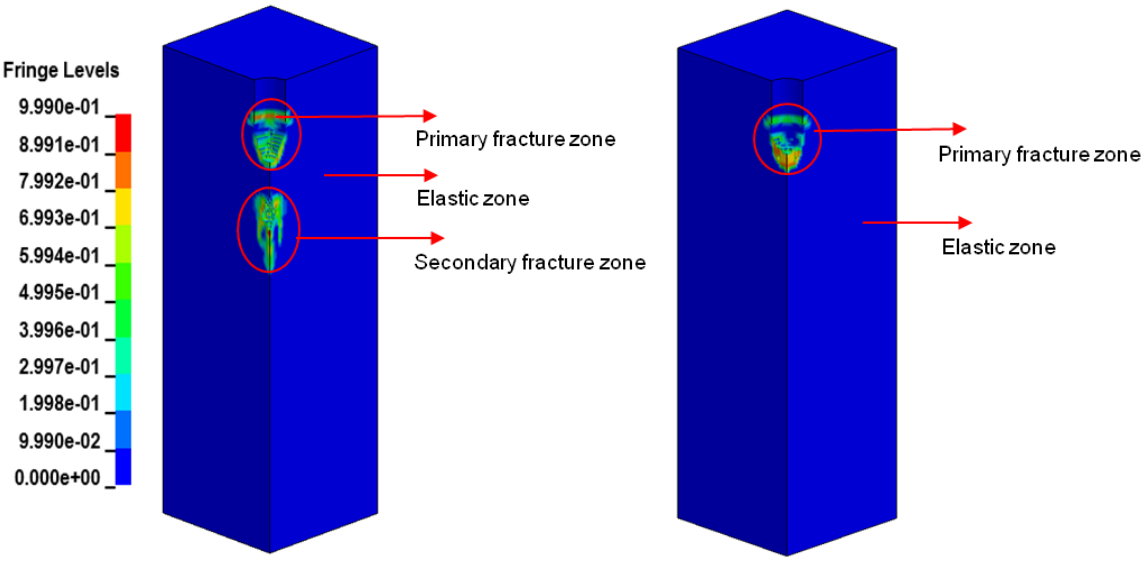

(*a*) loading period is 20 ms (*b*) loading period is 200 ms

Figure 8 The initial state of axial stress σ_y = 60 MPa and circumferential stress σ_x = σ_z = 10 MPa conducted at different loadings (Fringe levels are plastic strain)

Figure

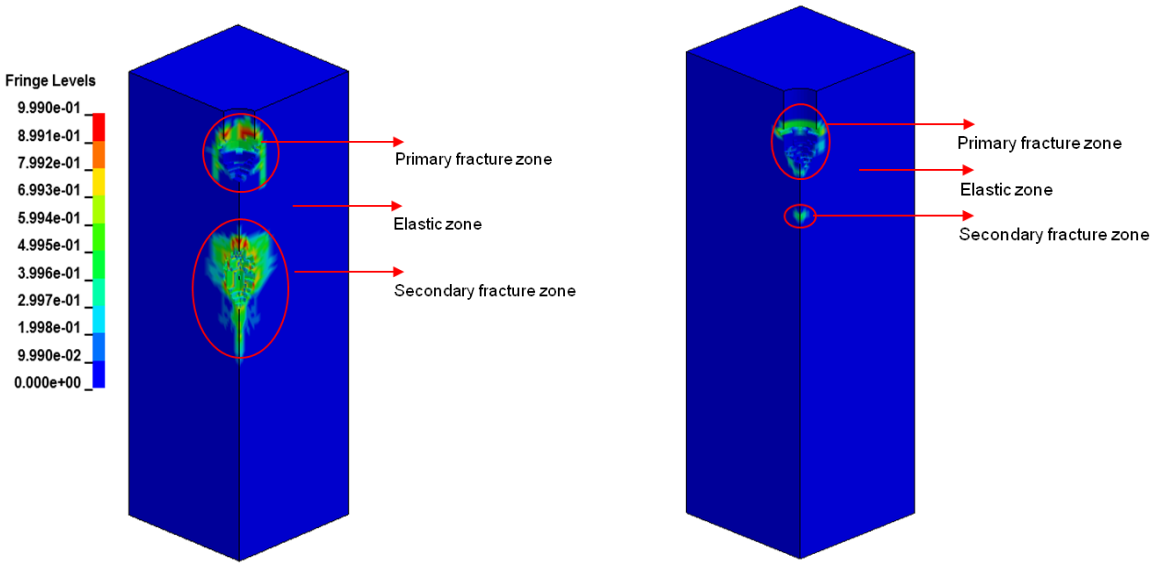

(*a*) σ_y=60 MPa, σ_x=σ_z=20 MPa, (*b*) σ_y=60 MPa, σ_x=σ_z=60 MPa

Figure 9 Characteristics of the rock response at the loading peak is 4 000 MPa (Fringe levels are plastic strain)

Figure

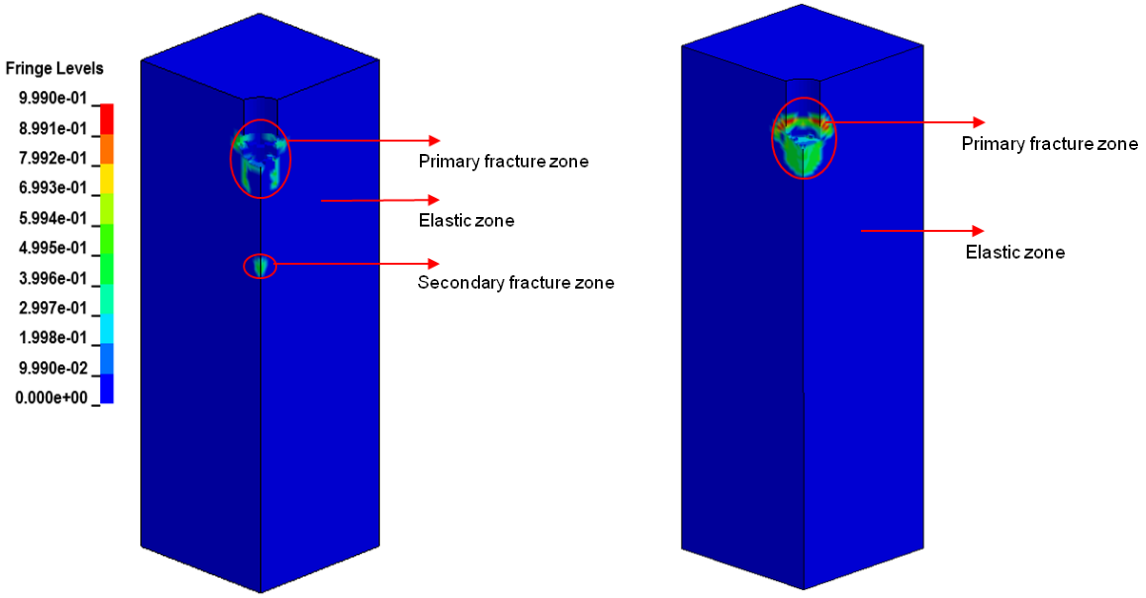

(*a*) σ_y=60 MPa, σ_x=σ_z=20 MPa, (*b*) σ_y=60 MPa, σ_x=σ_z=40 MPa

Figure 10 Characteristics of the rock response at the loading peak is 1 000 MPa (Fringe levels are plastic strain)

Figure

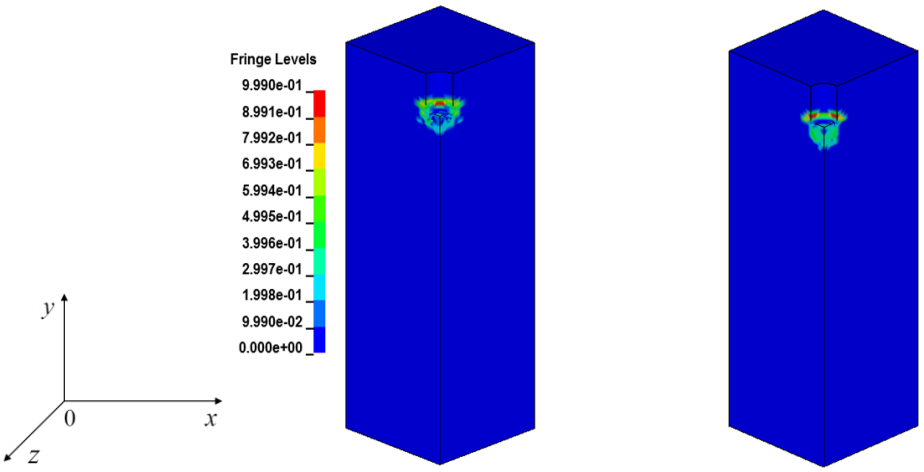

(a) Dynamic loading; (b) Quasi-static loading

Figure 11 Failure modes in front of the tunnel under different loading processes

(Fringe levels are plastic strain)

Figure

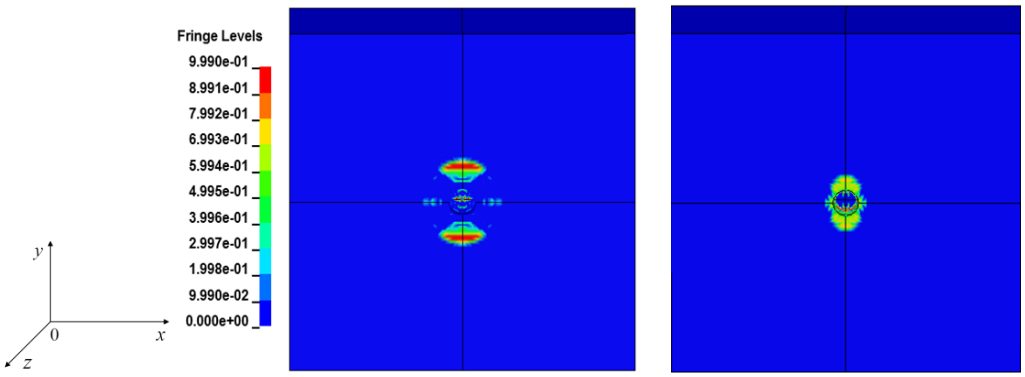

(a) Dynamic loading; (b) Quasi-static loading

Figure 12 Failure modes in circumference of the tunnel under different processes (Fringe levels are plastic strain)

Figure

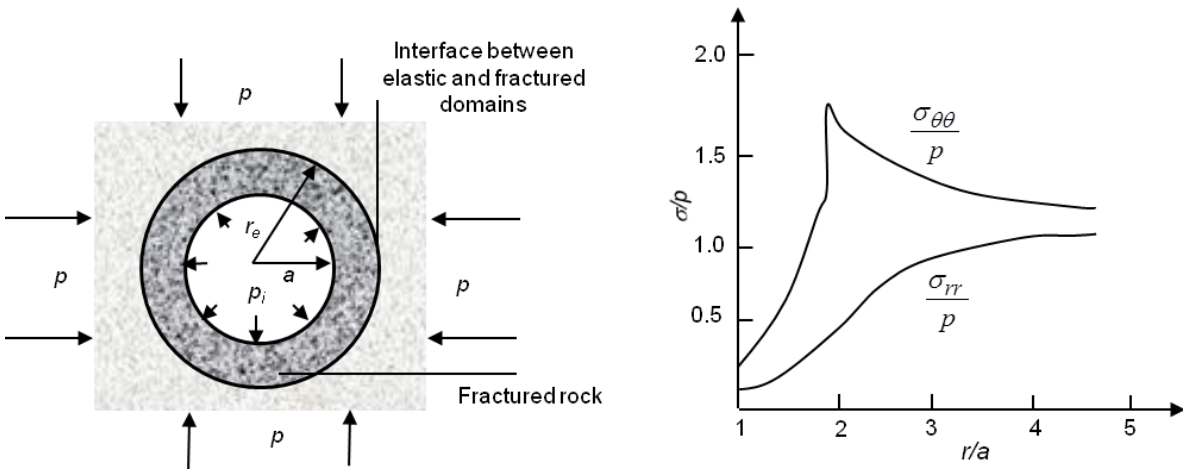

Figure 13 Stress distribution around a circular opening in a hydrostatic stress filed due to development of a fracture zone [17]

Figure

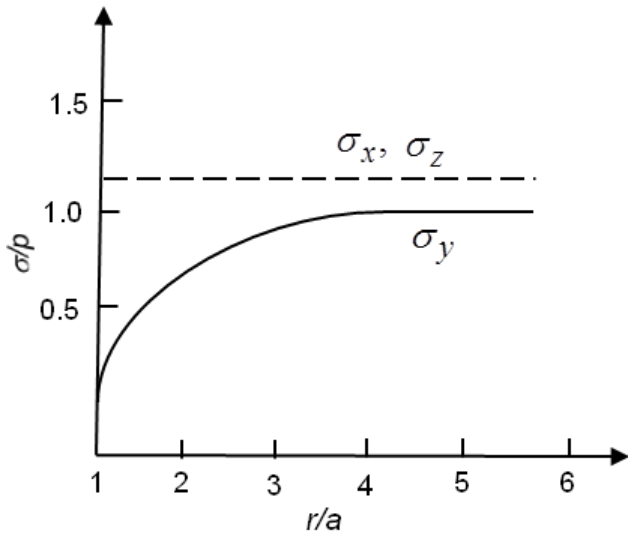

Figure 14 Sketch map of 3D stress state ahead of the working face

Figure

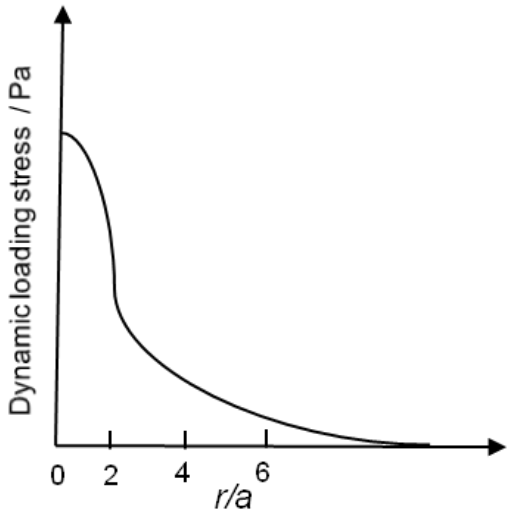

Figure 15 Dynamic loading magnitudes along the axial direction

Figure

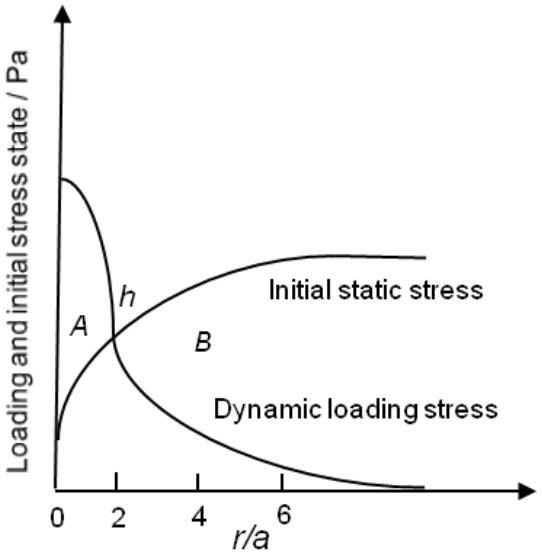

Figure 16 Coupled dynamic loading and initial static stress state

Figure

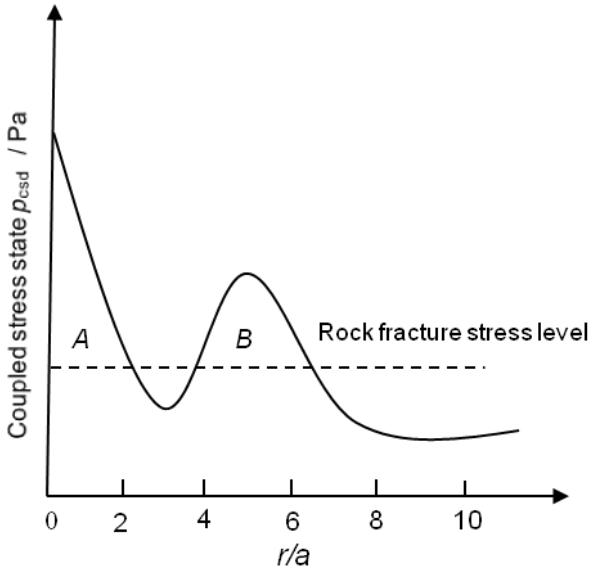

Figure 17 Sketch map of coupling result of impact loading and initial stress

Figure

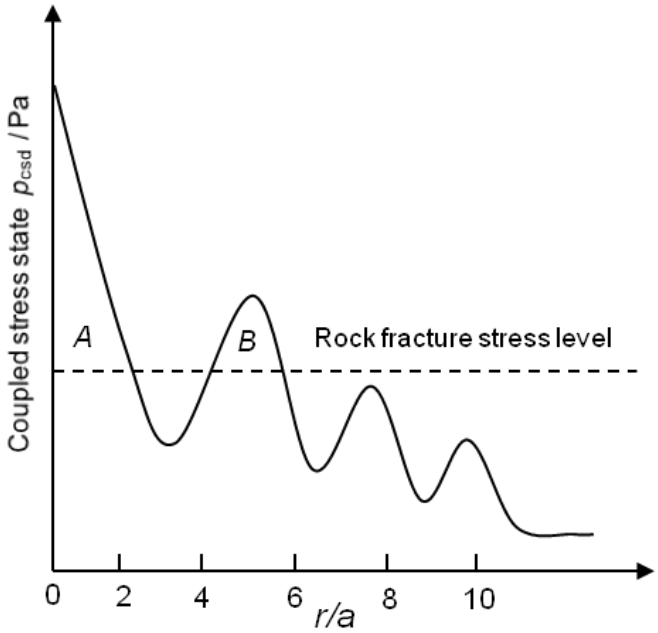

Figure 18 Sketch map of multiple peaks of coupling impact loading and initial stress

Figure

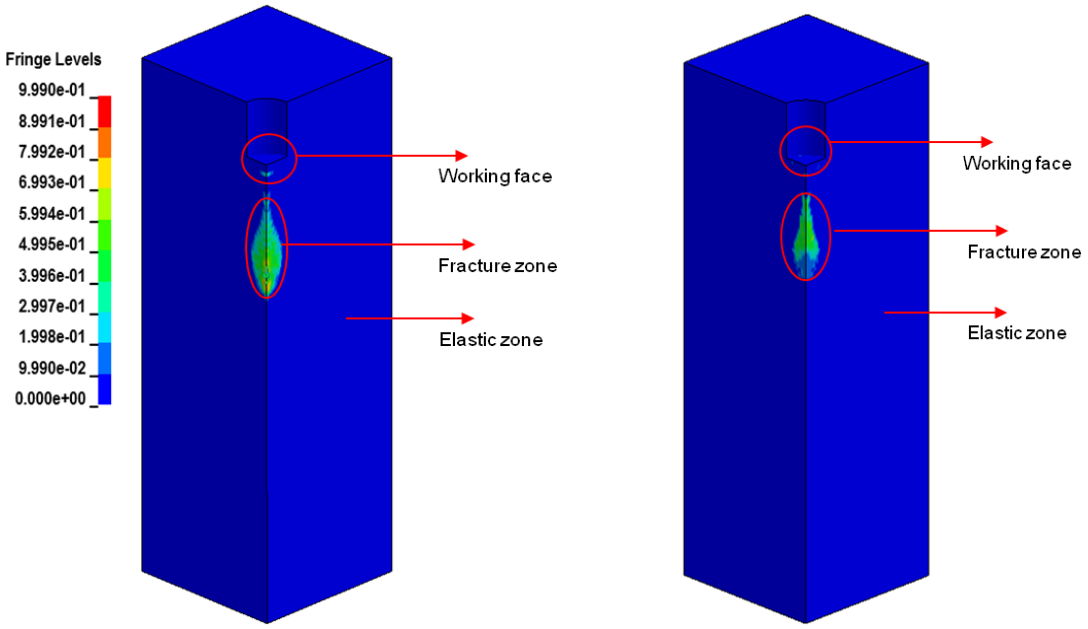

(*a*) σ_y=60 MPa, σ_x=σ_z=10 MPa, (*b*) σ_y=60 MPa, σ_x=σ_z=20 MPa

Figure 19 Fracture zone induced in far field (Fringe levels are plastic strain)

Table title

Table 1 Material properties of rock

Table

Table 1 Material properties of rock

PR	D/ (kg·m^{-3})	IFA /°	YM / GPa	UCS / MPa	UTS / MPa
0.19	2700	52	40	153	9.5

PR: Poisson's Ratio, D: Density, IFA: Internal Friction Angle, YM: Young's Modulus, UCS: Uni-axial Compression Strength, UTS: Uni-axial Tensile Strength.